

# A Comprehensive Ultrastructure and Transcriptome Analyses of Early Regeneration in *Ophryotrocha Xiamen* Sp. Nov. (Annelida: Dorvilleidae)

**Ruanni Chen**

Minjiang University

**Irum Mukhtar**

Minjiang University

**Shurong Wei**

Minjiang University

**Siyi Wu**

Minjiang University

**Jianming Chen** (✉ [chenjm@mju.edu.cn](mailto:chenjm@mju.edu.cn))

Minjiang University <https://orcid.org/0000-0003-0400-3092>

---

## Research article

**Keywords:** New species, *Ophryotrocha*, early regeneration, transcriptome, annelid

**Posted Date:** October 26th, 2020

**DOI:** <https://doi.org/10.21203/rs.3.rs-96086/v1>

**License:**   This work is licensed under a Creative Commons Attribution 4.0 International License.

[Read Full License](#)

---

# Abstract

## Background

In recent years, significant progress has been made using powerful genetic approaches with newly developed models for understanding on regeneration, however, the molecular and cellular basis of early regeneration remains unclear. Annelids of the genus *Ophryotrocha* have long been subjects of research use as model species in ecological, toxicological, reproductive, and regenerative investigations. Although, *Ophryotrocha* spp., are amenable to molecular, cellular, and functional analyses, still in need to explore new model organisms in this genus to understand regeneration mechanisms. Here, we focus on a newly identified *Ophryotrocha* species for its early regeneration developmental mode.

## Results

Based on detailed morphological (K-maxillae, rosette gland, and chromosome number) and molecular analyses, we present, *O. xiamen* as a new suitable model species to investigate the early regeneration mechanism. The comparative transcriptome analysis showed the gene expression patterns were related to transcriptional regulation, energy metabolism profiles and structure and signal transduction during early stages of regeneration. Data also exhibited that genes such as *neurotrypsin*, *Nos2*, *DMBT1*, *SCO spondin*, and *endotubin* associated to regulate inflammation, enterocyte differentiation, apoptosis, and neuroepithelial, were up-regulated during early regeneration stages (wound healing and blastema formation). Additionally, most of the known regeneration-related genes of annelids were also identified in *O. xiamen* which enabled to explore the precise functions of genes involved in regeneration process.

## Conclusions

This study enriches the identification of genus *Ophryotrocha* in Chinese coastal zones, an area with high abundances of annelids. The comparative transcriptome analysis provided the whole expression changes during early regeneration process. Morphology and molecular shred of evidences in *O. xiamen* revealed similar features of early regeneration with other invertebrates. Information on potential candidate genes associated with early regeneration in *O. xiamen*, will be useful for further studies.

## Background

Annelids of genus *Ophryotrocha* Claparede & Meczniow, 1869 are found worldwide from shallow to deep waters, including extreme habitats such as methane seeps, hydrothermal vents, aquaculture sites, and wood or whale falls [1-3]. More than 70 species in this genus have been formally described so far [4]. Due to the characteristic features such as short generation time, high fecundity, rapid individual growth rates and capable of laboratory maintenance, *Ophryotrocha* has been used as a model organism in several fields of comparative and evolutionary biology of marine invertebrates [1, 5].

The limited dispersal capability due to scant adult motility and lack of pelagic larvae may lead to the discontinuous distribution of *Ophryotrocha* species. Yet, some species show a rather continuous distribution on a regional scale [6]. In the past decades, many new *Ophryotrocha* species have been formally described, which indicates that the distribution of *Ophryotrocha* species could be wider and more continuous than that recognized today [1, 7-9]. The fact that some species are found solely in sea farming areas or on whalebones may be due to low sampling efforts [7]. Despite the increasing number of described species, our knowledge on the distribution of *Ophryotrocha* along with Chinese coastal zones is still incomplete. Thus, the detailed investigation on *Ophryotrocha* needs to be extended in China, not only to find new species that helped to improve the phylogeny of hitherto but also to explore other functions including the mechanisms of regeneration.

In many studies, annelids have been extensively explored regeneration capabilities with much fewer efforts to investigate on the molecular mechanisms to understand their regeneration and development. On the other hand, the mechanism of regeneration has been partially impeded by morphological and molecular differences among distantly related species such as hydra and planarians [10, 11]. In recent decades, dozens of studies have proven that almost each species of annelids owns segmental regeneration ability which made it to be an excellent group to study the regeneration mechanisms [12, 13]. The ability to regenerate segments in annelids after amputation varies from one species to another; however, anterior regeneration is less common than posterior regeneration which has been documented in many annelid groups [12, 14]. In *Ophryotrocha*, no evidence has been shown for the ability of anterior regeneration, although species such as *Ophryotrocha puerilis* and *O. notoglandulata* have been shown to regenerate posteriorly [15]. Furthermore, regeneration in annelids can be manifested as the combined mechanisms of epimorphosis and morphallaxis involving broad cellular, molecular, and developmental process. Although information on the mechanisms of regeneration remained unclear, a comparative transcriptome analysis and next-generation sequencing can help us to enhance our understanding in this area of research.

Herein, we describe the new species *Ophryotrocha xiamen* **sp. nov.** (*O. xiamen*) which has been successfully cultured in our laboratory for more than two years. Morphological and molecular analyses were conducted to characterize the species identity. Furthermore, we analyzed transcriptome data and ultrastructural features to compare the differences between the control group and the regeneration group after amputation, mainly focused on the early stages of regeneration. Additionally, regeneration-related genes have been investigated to reveal the common regeneration mechanisms existed among diverse species.

## Methods

### Culture and life cycle of *O. xiamen*

The specimens identified as *O. xiamen* was collected from Baicheng coast of Xiamen, Fujian Province, China in November 2017 (Additional file 1), kept in petri dishes with sterilized seawater and fed with

artificial diet (shrimp diet, Fuxing Feed Co., Ltd. Xiamen, China). The salinity, water temperature, and photoperiod were maintained at 23–25‰,  $24 \pm 1$  °C and 12 L: 12 D, respectively. To understand the life cycle of *O. xiamen*, newly laid egg clusters were transferred into new petri dishes with sterilized seawater in triplicate. The different stages of the life cycle were observed using a light microscope. For regeneration experiments, adult specimens were anesthetized in 10% MgCl<sub>2</sub> solution in artificial seawater and dissected at prostomium, peristomium, and the middle part of the body using a scalpel. The amputated parts were placed in petri plates, each contained artificial seawater.

For DNA or RNA extraction, cultures were kept without feeding for 3 days at a temperature of  $24 \pm 1$  °C to ensure the purity of the samples, rinsed 3 times with sterilized seawater containing penicillin G (100U/mL) and streptomycin (100mg/mL).

### DNA extraction and phylogenetic analysis

A TIANamp Marine Animals DNA Kit (DP324, Tiangen Biotech Co. Ltd., Beijing, China) was used to extract DNA from *O. xiamen* according to the manufacturer's instructions. The mitochondrial cytochrome C oxidase I (*COI*) [16] and nuclear histone 3 (*H3*) genes [17] were amplified using primers in Additional file 2. Amplification cycle conditions were as follows: 5 min at 94°C, followed by 32 cycles at 94°C for 30 s, 51°C (*COI*)/ 56°C (*H3*) for 30 s, 72°C for 30 s, and a final extension at 72°C for 10 min. PCR products were sequenced with the amplification primers in Shanghai Shenggong Co., Ltd. (Shanghai, China).

Both newly generated sequences of *COI* and *H3* in this study were aligned separately using ClustalW in MEGA5.05 with previously reported sequences in GenBank (Additional file 3). A total of 45 terminal taxa were used in phylogenetic the analyses, including *O. xiamen*, other 37 species from the genus *Ophryotrocha*, 7 species from other genera within *Dorvilleidae*, and rooted using *Eunice pennata*. The phylogenetic trees were constructed by the Maximum likelihood method (ML) using MEGA software (version 5.05), with bootstrap value of 1,000. For the ML analysis, the three molecular datasets were combined and run in jModelTest [18] with BIC, which suggested GTR+I+G as the best model.

### RNA extraction, library construction, and Illumina sequencing

Transversely (at the middle of the body) dissected worms (Ox t) were used to extract RNA after one day. As a control group (Ox c), non-dissected worms cultured under the same conditions as dissected worms used for extraction. Total RNA was extracted using MiniBEST Universal RNA Extraction Kit (TaKaRa, 9767) according to the manufacturer's instructions. Triplicate RNA isolations were merged into one sample. RNA degradation and contamination were monitored on 1% agarose gels, while, concentration and integrity of RNA were measured using a Qubit RNA Assay Kit in Qubit 2.0 Fluorometer (Life Technologies, CA, USA) and RNA Nano 6000 Assay Kit of the Agilent Bioanalyzer 2100 system (Agilent Technologies, CA, USA). The two mRNA-seq libraries were performed at Beijing Berry Genomics Co., Ltd. (Beijing, China) with a NEBNext Ultra RNA Library Prep Kit for Illumina (NEB, USA) following the manufacturer's recommendations. mRNA was purified from total RNA using poly-T oligo-attached

magnetic beads. Fragmentation was carried out using divalent cations under elevated temperature in NEBNext First Strand Synthesis Reaction Buffer (5x). Second strand cDNA synthesis was subsequently performed using DNA Polymerase I and RNase H. Remaining overhangs were converted into blunt ends via exonuclease/polymerase activities. After adenylation of 3' ends of DNA fragments, NEBNext Adaptor with hairpin loop structure were ligated to prepare for hybridization. In order to select cDNA fragments of preferentially 150~200 bp in length, the library fragments were purified with AMPure XP system (Beckman Coulter, Beverly, USA). Prior to PCR reaction, 3  $\mu$ L USER Enzyme (NEB, USA) was used with size-selected adaptor-ligated cDNA at 37°C for 15 min followed by 5 min at 95 °C. Then PCR was performed with Phusion High-Fidelity DNA polymerase, Universal PCR primers and Index (X) Primer. Amplified products were purified (AMPure XP system) and library quality was assessed on the Agilent Bioanalyzer 2100 system.

### Assembly of sequencing and gene annotation

The clustering of the index-coded samples was performed on a cBot Cluster Generation System using TruSeq PE Cluster Kit v3-cBot-HS (Illumina) according to the manufacturer's instructions. After cluster generation, the library preparations were sequenced on an Illumina NovaSeq platform and 150 bp paired-end reads were generated. Raw sequences were deposited to NCBI Short Read Archive (SRA) database (<http://www.ncbi.nlm.nih.gov/Traces/sra/>).

### Scanning electron microscopy (SEM) for morphology changes of regeneration

Specimen samples were prepared for SEM according to previous methods [19]. Living specimen (Ox t and Ox c) were washed thrice with sterilized seawater and suspended into 2.5% glutaraldehyde at 4 °C for 24 h and then transferred to a mixture of a saturated solution of HgCl<sub>2</sub> and 1% OsO<sub>4</sub> (4:1) at 4 °C for 10 min. All solutions mentioned above were diluted in sodium cacodylate buffer (pH 7.2) followed by specimen dehydration in a graded ethanol series, critical point drying, setting on aluminum stubs, and sputter-coating with platinum. Prepared samples were examined with a SEM JSM-6380LV (JEOL, Tokyo, Japan) at the Fujian Academy of Agricultural Sciences, Fuzhou, China.

## Results

### Morphological characteristics of *O. xiamen*

The adult *O. xiamen* with 24 segments, measuring  $3.10 \pm 0.44$  mm (n=15) long, were observed for detail morphological characteristics. The worm body is long, translucent while opaque white when preserved, segmented having longitudinal grooves in the middle segments, and dorso-ventrally flattened (Fig. 1 A, B). Jaws and paired light-reflecting eyes in the enlarged head can be observed under microscope. The head of adult *O. xiamen* (Fig. 1C) displaying paired digitiform antennae which surmounted with the curved cilia is similar with *O. labronica* and *O. japonica*. Dorsal and ventral bundles of cilia are presented throughout the body and formed complete rings on peristomium and pygidium (Fig. 1B), while the pygidium bearing two pygidial cirri (Fig. 1E) and median stylus only appeared in the larval stage. Based

on molecular analysis, we suggested that the diploid chromosome number of this species is  $2n=6$  chromosomes (Additional file 4).

The tube-shaped egg-cocoon of *O. xiamen* is found protected by the female to undergo direct development (Additional file 4) and each cocoon contains about 150-230 zygotes. Seven days after egg-laying, larvae with short pygidial stylus were released from the cocoon as two-segmented individuals at 25°C and further growth was achieved via adding new segments before the pygidium. They move around the bottom or the seawater surface using both parapodia and rings of cilia on the surface. Plenty of oocytes are concentrated in the middle and posterior regions of the coelom. The mandibles show no significant changes during the life-cycle while the maxillae moult to the K-maxillae (Additional file 4) since 12- to 15-segments. The moulting time is different between male and female, the changing occurred early in males. The first spawning was observed at 28 days. The life history events are given in Additional file 5.

### Phylogenetic analysis

The combined alignment consisted of 804 bps, of which *COI* had 524 bps and *H3* had 280 bps. Phylogenetic analyses resulted in similar tree topologies regardless of which tree reconstruction methods were used, therefore, only the results from the maximum likelihood analysis are discussed and shown (Fig. 2, Additional file 3). The phylogenetic tree showed that the new species *O. xiamen* positioned within the 'labronica' clade and indicating a close relationship with *O. notoglandulata* and *O. japonica* and concurred with morphological characters. The phylogeny of the species also agreed with the previous studies that *Exallopus jumarsi* and *Iphitime hartmanae* belonged to *Ophryotrocha* [20, 21].

### Morphological changes during early regeneration

The anterior and posterior regeneration abilities were investigated in the dissected body halves of the adult worms. Initially, internal organs and coelomic fluid were oozed out immediately after amputation. However, a rapid regeneration process was observed in the posterior half, while anterior half showed a slow regeneration. The detail of the regeneration stages after amputation is as follows: day 1; after amputation, epidermis and gut epithelia sealed amputated open surface just like typical healing by fusing with tissues, indicating that wound healing was already achieved, day 2; a tiny posterior protuberance was observed, day 3; as regeneration proceeded, growing protuberance increased in size, a complete-pygidium bearing with two pygidial cirri could be observed and eventually restored to a normal size (Fig. 3). During the first 3 days after amputation, the regeneration processes of different the amputation sites (segment 2, 4, 6, 10) were found to be similar without timing difference (not shown). Interestingly, we observed that *O. xiamen* could partially restore the anterior end. It was also observed that the ability to regenerate segments anteriorly was less promising than the posterior regeneration and no blastema was observed in early regeneration. Only part of prostomium or 1-2 anterior segments could be regenerated within two weeks (Additional file 6). Although the worms without peristomium could survive for months, they finally starved to death.

## Transcriptome overview

In total, 16.02 and 18.52 million raw reads were generated from amputated group (1 day) and control group of *O. xiamen*, respectively. After the removal of adaptor sequences, ambiguous reads and low-quality reads, a total of 23,712,145 reads comprising 7,099,167,646 bases from the untreated group and 24,034,889 reads comprising 7,195,652,874 bases from amputation group were obtained. In total, 72,980 unigenes were obtained with a mean length of 1180 bp, 41.1% GC content and an N50 of 1,976 bp. Based on the size distribution analysis, the lengths of 25,613 unigenes (35.1%) were > 1000 bp (Table 1).

Among them, 19,574, 3048, and 13,755 unigenes were matched in the NR, NT, and Swiss-Prot databases, respectively. More than 62.5% of unigenes possessed an E-value of more than  $1e^{-30}$ . Of the database proteins that matched predicted proteins, *O. xiamen* unigenes had the highest hits to *Capitella teleta* (20.9%), a polychaeta worm, followed by *Lingula anatina* (16.2%) (Additional file 7).

For functional predictions and categories, all 8788 unigenes were annotated with 6,980 Gene ontology (GO) terms and assigned into three functional GO terms, including cellular component (452 subcategories), molecular function (180 subcategories), and biological process categories (2114 subcategories). Cell (4100 unigenes) and cell part (3958 unigenes) were the main sub-categories in the cellular component category, while the main sub-categories in molecular function were catalytic activity (3344 unigenes) and binding (3271 unigenes), and the major biological process was cellular process (4944 unigenes).

## Comparative gene expression during regeneration

To identify the differentially expressed genes (DEGs) involved in regeneration processes, genes expressions were compared and selected between control and regeneration groups using a statistical cutoff of fold change >2 and FDR < 0.05. The hierarchical clustering heatmap was generated to represent the up- and down-regulated genes. A total of 243 genes could be detected, including 50 up regulated and 193 down regulated (Fig. 4, Additional file 8). Among up regulated genes, 17 with significant up regulated genes were annotated as *neurotrypsin*, *nitric oxide synthase 2 (Nos2)*, *deleted in malignant brain tumors 1 (DMBT1)*, *SCO spondin*, *endotubin*, *18S rRNA* and *28S rRNA* might be the key elements during early regeneration (Table 2). Large scale of unknown genes was also found to have significantly different expression level, which indicated that the process of regeneration might involve some new genes. Thus, further study of novel genes could help to disclose the mechanisms of early regeneration.

After the data analysis, the DEGs between treated and control groups were classified into 124 GO subcategories (78 subcategories for biological process, 26 subcategories for molecular function, and 20 subcategories for cellular component,  $p < 0.01$ ). Translation, structural constituent of ribosome, ribosome and intracellular ribonucleoprotein complex subcategories contained the most DEGs and would be treated as the focus of analysis (Fig. 5). To further explore the mechanisms of regeneration, the DEGs were mapped to 132 KEGG Orthology (KO). Among them, DEGs enriched in ribosome, oxidative phosphorylation, parkinson's disease, and cardiac muscle contraction pathways which were related to

transcriptional regulation and energy metabolism profiles represented the largest groups. While DEGs involved in pathogenic *Escherichia coli* infection, arrhythmogenic right ventricular cardiomyopathy (ARVC), salmonella infection, Huntington's disease, Alzheimer's disease, and Hippo signaling pathways were related to structure and signal transduction. The most abundant 20 differentially expressed signaling pathways have been listed (Additional file 9).

### Candidate genes involved in regeneration process

In order to explore the mechanism of early regeneration, the putative genes that have been implicated in other regeneration models were identified using BLAST searches (Additional file 10). A total of 130 regeneration-related candidates were found in this study. Among these genes, *brachyury*, *cyclinB*, *Hox A2*, *indian hedgehog*, *myc*, *notch1*, *notch4*, *PRDM8*, and *PRDM9* were found up regulated, while *notch2*, *neurogenin*, *matrix metalloproteinase*, and *glutamine synthetase* were detected to be down-regulated ( $|\log_{2}FC| > 1$ ). Only *cyclin B* showed significant increased expression in early regeneration ( $|\log_{2}FC| > 1$ , FDR < 0.05). Genes, such as *Hox*, *notch*, *paired box protein*, *PRDM*, *tudor domain-containing (tdrd)* and *wnt*, with multiple isoforms were also founded, indicating that these might exist as multiple unique homologs and involved in new functions during the early regeneration.

## Discussion

In the present study, *Ophryotrochaxiamen* is identified to be a new species of *Ophryotrocha*. The globally distributed *Ophryotrocha* species are a well-studied group of marine polychaetes and part of them have been used as models in ecological, toxicological, reproductive, and regenerative studies [2, 22, 23]. Due to the opportunistic and stress tolerant characters, more new species yet to be discovered worldwide [9]. Till to date, a limited number of species have been recorded in the diverse climatic and topographic coastal zones of China which contains a lot of unknown annelids still to be explored. The *O. xiamen*, previously collected from Baicheng the coast of Xiamen, could survive in the pressures up to 30Mpa, indicated that this species might have a wider distribution (unpublished observations). To establish confirmed taxonomic position, the identity of this species is revised based on the molecular tools combined morphological characters [1, 24].

Molecular identification of species based on conserved genes (other than ITS regions) sequencing, have been proved to be effective in elucidating phylogeographical structure and underlying evolutionary history in Polychaeta [6, 7]. In the present study, new molecular evidences, based on *COI* and *H3* sequences were obtained for the taxonomic position of *O. xiamen*. Phylogenetic analysis enabled us to distinguish *O. xiamen* from other species of *Ophryotrocha*. As an agreement with the previous studies, tree topology showed four distinct clades in *Ophryotrocha* that represents labronica, gracilis/hartmannae, lobifera and an undefined clade. The 'labronica' clade, including *O. xiamen*, is characterized by the diploid chromosome number of  $2n=6$ , similar external morphology, rosette glands, and K-maxillae [2, 25, 26]. Besides, the female would take care of its egg-cocoon till hatching and this phenomenon seemed universal in *Ophryotrocha* [27]. We also noticed that the adults could produce a network of mucous trails



which might be recognized by conspecifics. Within Annelida, the mucus, constitutes key factors in tube building, egg protection, and prevention of proliferation of pathogenic microorganisms making it a particularly attractive class of biocidal agents [28].

In some studies, it has already advocated that new models which amenable to molecular, cellular, and functional analyses is required to better understand the mechanisms of regeneration [29, 30]. Based on current study findings, *O. xiamen* seemed to be a particularly appropriate model to study the mechanism of regeneration.

The rapid posterior regeneration process which followed a reproducible path and timeline, allowing us to explore changes at different time points. Like in *Platynereis dumerilii* [31], the whole process in *O. xiamen* was also subdivided into two continuous phases, regeneration *per se* (first 3 days) and post-regenerative growth. In annelids, epimorphosis is common mode of posterior regeneration and often involves the formation of a blastema which composed of an outer sheet of epithelial cells and an inner mass of mesenchyme-like cells and finally form a completely posterior part. Our results showed that the amputated part could add new segments posteriorly and finally grow to its original size. This phenomenon has been explained that the worm was able to 'sense' the site that had been cut and adjust their amount accordingly [31]. In particular, no anterior segment regeneration was reported and the anterior regeneration occurred only when part of the prostomium remained intact. However, in this study, we observed that *O. xiamen* could form one or two new segments forward but no complete head region, including eye and antennae. Presumably, the lower percentage of successful regenerates in anterior regeneration can be attributed to the need for restoration of more complex structures including the brain, eye, and jaw [12, 26, 32]. Further work is needed to better understand the essential foundation for future mechanistic and comparative studies of regeneration.

The regeneration process was a complex morphological change, while only 243 transcripts with significantly differing transcript levels were found in *O. xiamen*. This could be explained by findings in other annelid that genes involved in the regeneration and normal growth process were largely overlapping and have been demonstrated to have similar expression patterns [31, 33, 34]. Among these, genes annotated as *neurotrypsin*, *Nos2*, *DMBT1*, *SCO spondin*, *endotubin*, *18S rRNA*, and *28S rRNA* were significantly up-regulated. During regeneration process, neurotrypsin and SCO-spondin are thought to be crucial for cognitive brain functions and regulate the balance between neuroepithelial proliferation and differentiation, respectively [35, 36]. Both DMBT1 and endotubin are required for enterocyte morphogenesis and differentiation [37, 38]. DMBT1 is also known as a protein with functions in innate immunity, inflammation, and angiogenesis by influencing proliferation, migration, and adhesion of endothelial cells [38, 39]. Previous study showed that *Nos2* was involved in Wnt/ $\beta$ -catenin signaling pathway which was crucial for early segmental regeneration [40]. In the early stages of regeneration, inflammation and apoptosis factors launch the downstream process of development [41, 42]. All of them were reported to play important roles in early embryonic development which contained several genes playing integral roles in re-specification of regenerated structures in several annelid species [14]. Due to the scarcity of annelid genomic data used for annotation, a large set of potentially novel DEGs in *O.*

*xiamen* were identified. Previous studies also revealed that unknown genes which showed similar expression trends with key regulators might be important and required during regeneration process. Thus, a well annotated genome data of *O. xiamen* which is already in progress are needed to explain the exact gene functions and roles in regeneration mechanisms.

To further the understanding of regeneration mechanisms in annelids, it will be of particular importance to identify genes that are specifically related to this process. By using BLAST searches, we found regeneration-related or putative genes that have been implicated in regeneration in other regeneration models [43]. All these genes have been reported involving in regenerative processes, including wound healing, blastema formation, controlling cell proliferation and morphogenesis [31, 33, 44]. Among these potential candidate genes, only *cyclin B* was significantly differentially expressed. Only one type of *cyclin B* was present in *O. xiamen*. Several studies indicated that the function of cyclin B protein in invertebrates might have a dual role as cyclin B1 and cyclin B2 which was suggested to participate in the reorganization of different aspects of the cellular architecture at mitosis and different functions in the cell cycle [45, 46]. In the early regeneration stage, wound healing and formation of the blastema, are a rapid process in annelids that consists of muscular contraction and epithelium formation [47]. Thus, the cyclin B in *O. xiamen* was suggested to have same functions in regulating the cell cycle during early regeneration. Meanwhile, other regeneration-related DEGs (fold change >2) including *glutamine synthetase*, *brachyury*, *Hox A2*, *indian hedgehog*, *matrix metalloproteinase*, *myc*, *neurogenin*, *notch 1/2/4*, and *PRDM8/9*, were already shown to be expressed during early regeneration stages in other annelids [31, 33, 48, 49]. Genes, such as *frizzled*, *notch*, *PRDM*, and *wnt*, were represented by multiple isogroups, likely indicating multiple unique homologs in *O. xiamen*, which is consistent with what is known about these gene families in other annelids [11, 44, 50]. Based on plenty of cellular level researches, molecular level studies are in need to provide a complete understanding of regenerative processes.

## Conclusions

In this study, *O.xiamen* has been identified to be a new species and a particularly appropriate model to study the mechanism of regeneration. We provide a detailed phylogenetic background, description of the morphology and regeneration process for this new species, a pre-requisite for any type of evolutionary study. Moreover, the comparative transcriptome analysis provides the whole expression changes during the early regeneration of this species. Morphology and molecular evidence in *O.xiamen* also revealed similar features of early regeneration with other invertebrates. Genes involved in regeneration have also been investigated to reveal the similarity in regeneration mechanisms among diverse species. We hope that further investigations based on *O. xiamen* as an alternative new model will provide deep insights into the regeneration process at morphological and molecular levels and will stimulate interest in evolutionary research.

## Abbreviations

ARVC: arrhythmogenic right ventricular cardiomyopathy; COI: Cytochrome C oxidase I; DMBT: Deleted in malignant brain tumors; FDR: False discovery rate; H3: Histone 3; Nos: Nitric oxide synthase; PRDM: PR domain; TDRD: tudor domain-containing

## Declarations

### Ethics approval and consent to participate

Not applicable.

### Consent for publication

Not applicable.

### Competing interests

The authors declare that they have no competing interests.

### Availability of data and materials

Raw Illumina sequences were deposited in the National Center for Biotechnology Information (NCBI) and can be accessed in the Short Read Archive (SRA) database (<http://trace.ncbi.nlm.nih.gov/Traces/sra/>) under accession numbers: SRR12074689 and SRR12074688. All the datasets supporting the results of this article are included within the article and its Additional files.

### Funding

This study was financially supported by China Ocean Mineral Resources Research and Development Association Program (Grant No. DY135-B2-13), the Project of Education Department of Fujian Province (Grant No. JAT190631) and Program for Innovative Research Team in Science and Technology of Education Department of Fujian Province, Project of Minjiang University (Grant No. MYK19003), and Project of Department of Fujian Science and Technology and in Fujian Province (Grant No. 2018N2001). Funding bodies had no role in the design of the study and collection, analysis, and interpretation of data and in writing the manuscript.

### Acknowledgements

The authors thank Aurora Genran Tao and Karlie Yuran Chen for helping in sampling and for culturing this new species. We thank the Fujian academy of agricultural sciences for sample preparation.

### Authors' Contributions

RC and JC planned and designed the research. SW<sub>1</sub> and SW<sub>2</sub> prepared the sample. RC performed experiments and analyzed data. RC, JC, and IM wrote and modified the manuscript. All authors have read

and approved the manuscript.

## References

1. Ravara A, Marçal AR, Wiklund H, Hilário A. First account on the diversity of *Ophryotrocha* (Annelida, Dorvilleidae) from a mammal-fall in the deep-Atlantic Ocean with the description of three new species. *Systematics and Biodiversity*. 2015;13(6):555-570.
2. Dahlgren TG, Akesson B, Schander C, Halanych KM, Sundberg P. Molecular phylogeny of the model annelid *Ophryotrocha*. *The Biological Bulletin*. 2001;201(2):193-203.
3. Wiklund H, Glover AG, Dahlgren TG. Three new species of *Ophryotrocha* (Annelida: Dorvilleidae) from a whale-fall in the North-East Atlantic. *Zootaxa*. 2009;2228(1):43-56.
4. Read GF, Fauchald K. (Ed.). World Polychaeta database. Accessed at <http://www.marinespecies.org/polychaeta> on 2020-09-17.
5. Lorenzi MC, Schleicherová D, Sella G. Life history and sex allocation in the simultaneously hermaphroditic polychaete worm *Ophryotrocha diadema*: the role of sperm competition. *Integrative and Comparative Biology*. 2006;46(4):381-389.
6. Cossu P, Maltagliati F, Pannacciulli FG, Simonini R, Massamba-N'Siala G, Casu M, et al. Phylogeography of *Ophryotrocha labronica* (Polychaeta, Dorvilleidae) along the Italian coasts. *Marine Ecology*. 2015;36(4):1088-1097.
7. Salvo F, Wiklund H, Dufour SC, Hamoutene D, Pohle G, Worsaae K. A new annelid species from whalebones in Greenland and aquaculture sites in Newfoundland: *Ophryotrocha cyclops* sp. nov. (Eunicida: Dorvilleidae). *Zootaxa*. 2014;3887(5):555-568.
8. Jimi N, Taru M, Imura S. Life in the city: a new scavenger species of *Ophryotrocha* (Annelida, Dorvilleidae) from Odaiba, Tokyo, Japan. *Proceedings of the Biological Society of Washington*. 2019;132(1):131-140.
9. Paxton H, Åkesson B. The *Ophryotrocha labronica* group (Annelida: Dorvilleidae)-with the description of seven new species. *Zootaxa*. 2010;2713(1):1-24.
10. Galliot B, Chera S. The Hydra model: disclosing an apoptosis-driven generator of Wnt-based regeneration. *Trends in Cell Biology*. 2010;20(9):514-523.
11. Kao D, Felix D, Aboobaker A. The planarian regeneration transcriptome reveals a shared but temporally shifted regulatory program between opposing head and tail scenarios. *BMC Genomics*. 2013;14(1):797.
12. Bely AE. Distribution of segment regeneration ability in the Annelida. *Integrative and Comparative Biology*. 2006;46(4):508-518.
13. Özpölat BD, Bely AE. Developmental and molecular biology of annelid regeneration: a comparative review of recent studies. *Current Opinion in Genetics and Development*. 2016;40:144-153.
14. Martinez-Acosta VG, Zoran MJ. Evolutionary aspects of annelid regeneration. *eLS*. 2015;1-7.

15. Pfannenstiel HD. Regeneration in the gonochoristic polychaete *Ophryotrocha notoglandulata*. Marine Biology. 1974;24(3):269-272.
16. Folmer O, Black M, Hoeh W, Lutz R, Vrijenhoek R. DNA primers for amplification of mitochondrial cytochrome c oxidase subunit I from diverse metazoan invertebrates. Molecular Marine Biology and Biotechnology. 1994;3(5):294-299.
17. Donald J, Colgan WFP, Peter E, Eggle. Gastropod evolutionary rates and phylogenetic relationships assessed using partial 28S rDNA and histone H3 sequences. Zoologica Scripta. 2000;29(1):29-63.
18. Posada D. jModelTest: phylogenetic model averaging. Molecular Biology and Evolution. 2008;25(7):1253-1256.
19. Chen R, Mao Y, Wang J, Liu M, Qiao Y, Zheng L, et al. Molecular mechanisms of an antimicrobial peptide piscidin (Lc-pis) in a parasitic protozoan, *Cryptocaryon irritans*. BMC Genomics. 2018;19(1):192.
20. Sergi Taboada HW, Adrian G, Glover, Thomas G, Dahlgren, Javier Cristobo, Conxita Avila. Two new Antarctic *Ophryotrocha* (Annelida: Dorvilleidae) described from shallow-water whale bones. Polar Biology. 2013;36(7):1031-1045.
21. Helena Wiklund IVA, Adrian G, Glover, Craig R, Smith, Amy R, Baco, Thomas G, Dahlgren. Systematics and biodiversity of *Ophryotrocha* (Annelida, Dorvilleidae) with descriptions of six new species from deep-sea whale-fall and wood-fall habitats in the north-east Pacific. Systematics and Biodiversity. 2012, 10(2):243-259.
22. Mercier A, Baillon S, Hamel JF. Life history and seasonal breeding of the deep-sea annelid *Ophryotrocha* sp. (Polychaeta: Dorvilleidae). Deep Sea Research Part I: Oceanographic Research Papers. 2014;91:27-35.
23. Cassai C, Prevedelli D. Fecundity and reproductive effort in *Ophryotrocha labronica* (Polychaeta: Dorvilleidae). Marine Biology. 1999;133(3):489-494.
24. Elgetany AH, El-Ghobashy AE, Ghoneim A, Struck TH. Description of a new species of the genus *Marphysa* (Eunicidae), *Marphysa aegypti* sp. n., based on molecular and morphological evidence. Invertebrate Zoology. 2018;15(1):71-84.
25. Paxton H, Åkesson B: Redescription of *Ophryotrocha puerilis* and *O. labronica* (Annelida, Dorvilleidae). Marine Biology Research. 2007;3(1):3-19.
26. Macnaughton MO, Worsaae K, Eibye-Jacobsen D. Jaw morphology and ontogeny in five species of *Ophryotrocha*. Journal of Morphology. 2010;271(3):324-339.
27. Maynard SJ. Parental investment: A prospective analysis. Animal Behaviour. 1977;25:1-9.
28. Stabili L, Schirosi R, Licciano M, Giangrande A. Role of *Myxicola infundibulum* (Polychaeta, Annelida) mucus: From bacterial control to nutritional home site. Journal of Experimental Marine Biology and Ecology. 2014;461:344-349.
29. Sánchez AA. To solve old problems, study new research organisms. Developmental Biology. 2018;433(2):111.

30. Grillo M, Konstantinides N, Averof M. Old questions, new models: unraveling complex organ regeneration with new experimental approaches. *Current Opinion in Genetics and Development*. 2016;40:23-31.
31. Planques A, Malem J, Parapar J, Vervoort M, Gazave E. Morphological, cellular and molecular characterization of posterior regeneration in the marine annelid *Platynereis dumerilii*. *Developmental Biology*. 2019;445(2):189-210.
32. Chen CP, Fok SK-W, Hsieh YW, Chen CY, Hsu FM, Chang YH, et al. General characterization of regeneration in *Aeolosoma viride* (Annelida, Aeolosomatidae). *Invertebrate Biology*. 2020;139(1):e12277.
33. Ribeiro RP, Ponz-Segrelles G, Bleidorn C, Aguado MT. Comparative transcriptomics in Syllidae (Annelida) indicates that posterior regeneration and regular growth are comparable, while anterior regeneration is a distinct process. *BMC Genomics*. 2019;20(1):855.
34. Gazave E, Béhague J, Laplane L, Guillou A, Préau L, Demilly A, et al. Posterior elongation in the annelid *Platynereis dumerilii* involves stem cells molecularly related to primordial germ cells. *Developmental Biology*. 2013;382(1):246-267.
35. Reif R, Sales S, Dreier B, Lüscher D, Wölfel J, Gisler C, et al. Purification and enzymological characterization of murine neurotrypsin. *Protein Expression and Purification*. 2008;61(1):13-21.
36. Vera A, Recabal A, Saldivia N, Stanic K, Torrejón M, Montecinos H, et al. Interaction between SCOP and low density lipoproteins from embryonic cerebrospinal fluid modulates their roles in early neurogenesis. *Frontiers in Neuroanatomy*. 2015;9:72.
37. Cox CM, Lu R, Salcin K, Wilson JM. The endosomal protein endotubin is required for enterocyte differentiation. *Cellular and Molecular Gastroenterology and Hepatology*. 2018;5(2):145-156.
38. Müller H, Nagel C, Weiss C, Mollenhauer J, Poeschl J. Deleted in malignant brain tumors 1 (DMBT1) elicits increased VEGF and decreased IL-6 production in type II lung epithelial cells. *BMC pulmonary medicine*. 2015;15(1):32.
39. Müller H, Hu J, Popp R, Schmidt MH, Müller-Decker K, Mollenhauer J, et al. Deleted in malignant brain tumors 1 is present in the vascular extracellular matrix and promotes angiogenesis. *Arteriosclerosis, Thrombosis, and Vascular Biology*. 2012;32(2):442-448.
40. Du Q, Park KS, Guo Z, He P, Nagashima M, Shao L, et al. Regulation of human nitric oxide synthase 2 expression by Wnt  $\beta$ -catenin signaling. *Cancer Research*. 2006;66(14):7024-7031.
41. Qin YF, Fang HM, Tian QN, Bao ZX, Lu P, Zhao JM, et al. Transcriptome profiling and digital gene expression by deep-sequencing in normal/regenerative tissues of planarian *Dugesia japonica*. *Genomics*. 2011;97(6):364-371.
42. Goessling W, North TE, Loewer S, Lord AM, Lee S, Stoick-Cooper CL, et al. Genetic interaction of PGE2 and Wnt signaling regulates developmental specification of stem cells and regeneration. *Cell*. 2009;136(6):1136-1147.
43. Zhao M, Rotgans B, Wang T, Cummins S. REGene: a literature-based knowledgebase of animal regeneration that bridge tissue regeneration and cancer. *Scientific Reports*. 2016;6:23167.

44. Nyberg KG, Conte MA, Kostyun JL, Forde A, Bely AE. Transcriptome characterization via 454 pyrosequencing of the annelid *Pristina leidy*, an emerging model for studying the evolution of regeneration. *BMC Genomics*. 2012;13(1):287.
45. Qiu L, Jiang S, Zhou F, Huang J, Guo Y. Molecular cloning and characterization of a cyclin B gene on the ovarian maturation stage of black tiger shrimp (*Penaeus monodon*). *Molecular Biology Reports*. 2007;1-8.
46. Han K, Dai Y, Zou Z, Fu M, Wang Y, Zhang Z. Molecular characterization and expression profiles of cdc2 and cyclin B during oogenesis and spermatogenesis in green mud crab (*Scylla paramamosain*). *Comparative Biochemistry and Physiology Part B: Biochemistry and Molecular Biology*. 2012;163(3-4):292-302.
47. Bely AE. Early events in annelid regeneration: a cellular perspective. *Integrative and Comparative Biology*. 2014; 54(4):688-699.
48. Kitakoshi T, Shimizu T. An oligochaete homologue of the Brachyury gene is expressed transiently in the third quartette of micromeres. *Gene Expression Patterns*. 2010;10(6):306-313.
49. Miao T, Wan Z, Sun L, Li X, Xing L, Bai Y, et al. Extracellular matrix remodeling and matrix metalloproteinases (ajMMP-2 like and ajMMP-16 like) characterization during intestine regeneration of sea cucumber *Apostichopus japonicus*. *Comparative Biochemistry and Physiology Part B: Biochemistry and Molecular Biology*. 2017;212:12-23.
50. Cho SJ, Vallès Y, Giani Jr VC, Seaver EC, Weisblat DA. Evolutionary dynamics of the wnt gene family: a lophotrochozoan perspective. *Molecular Biology and Evolution*. 2010;27(7):1645-1658.

## Tables

**Table 1** Quality parameters of illumine transcriptome sequencing of *O. xiamen*.

<b>Data generation and filtering</b>	
Total number	72,980
Total length	86,140,670
GC content (%)	49.92
<b>Assembly statistics</b>	
300–1,000(bp)	38,088 (44.28%)
1,000–3,000 (bp)	19,941 (23.18%)
>3,000 (bp)	9,970 (11.59%)
Unigenes	86,017
Total length (bp)	83,647,650
N50 length (bp)	1,505
Mean length (bp)	972.41

**Table 2** List of significantly up-regulated genes in early regeneration of *O. ximen*.



GeneID	Annotation	logFC	pValue	FDR
TRINITY_DN51273_c0_g1	Deleted in malignant brain tumors1 (DMBT1)	3.037675	4.57E-05	0.015983
TRINITY_DN50786_c0_g1	Neurotrypsin	3.1618	9.29E-06	0.003945
TRINITY_DN55189_c1_g3	Nitric oxide synthase 2 (Nos2)	3.184915	8.04E-06	0.003433
TRINITY_DN43190_c0_g1	Monocarboxylate transporter 12	3.20869	8.96E-05	0.028707
TRINITY_DN51913_c0_g1	SCO spondin like	3.270135	5.18E-06	0.002397
TRINITY_DN50786_c0_g2	Apical endosomal glycoprotein	3.393203	2.68E-06	0.001388
TRINITY_DN55867_c1_g3	ncRNA	3.454196	2.06E-05	0.007981
TRINITY_DN53819_c1_g1	16S rRNA	3.841241	7.55E-06	0.003307
TRINITY_DN46494_c2_g1	28S rRNA	4.584054	3.50E-07	0.000258
TRINITY_DN50002_c0_g2	16S rRNA	4.886075	6.91E-05	0.023013
TRINITY_DN44012_c2_g2	28S rRNA	4.934653	3.60E-07	0.00026
TRINITY_DN44852_c0_g1	18S rRNA	5.806989	1.86E-09	2.93E-06
TRINITY_DN56797_c1_g1	18S rRNA	5.822492	1.69E-09	2.73E-06
TRINITY_DN55100_c4_g4	28S large subunit rRNA	6.03928	1.63E-07	0.000133
TRINITY_DN55100_c4_g6	28S rRNA	7.551671	0.000126	0.037895
TRINITY_DN46867_c0_g1	rRNA promoter binding protein	8.690415	4.00E-07	0.000278
TRINITY_DN44852_c0_g2	18S rRNA	9.049187	5.90E-08	5.49E-05

List contains only 17 annotated unigenes (fold change >2 and FDR < 0.05). The unknown genes are not shown.

## Figures

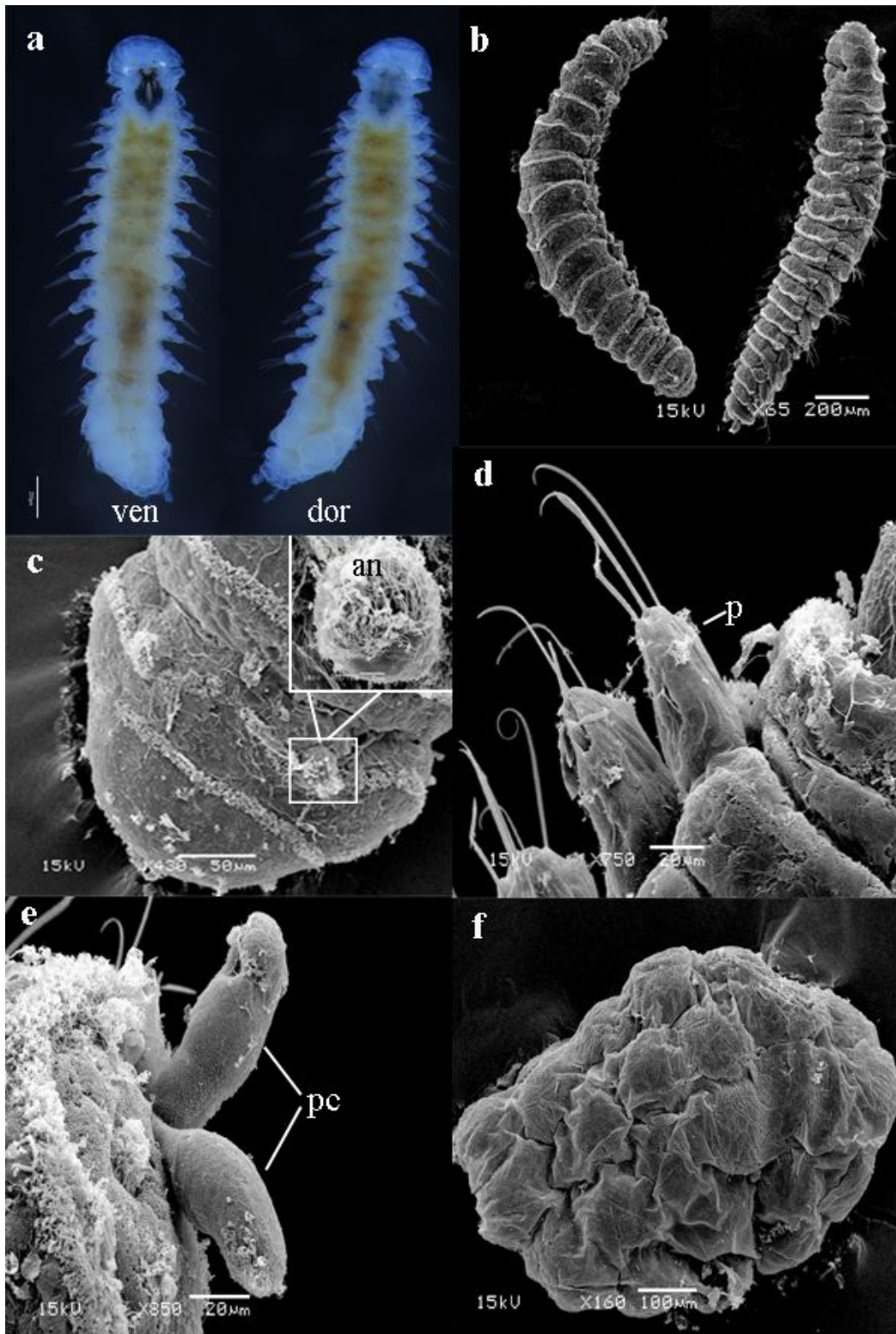


**Figure 1**

*Ophryotrocha xiamen*, sp. nov.. a Living adult of *O. Xiamen*. b SEM image of *O. xiamen*. c Head region with paired antennae. d Median parapodia of *O. xiamen*. e Pygidium with anal cirrus. f Egg-cocoon. ven: ventral view; dor: dorsal view; an: antennae; p: parapodia; pc: pygidial cirri. Scale bars were showed in the bottom of each images.

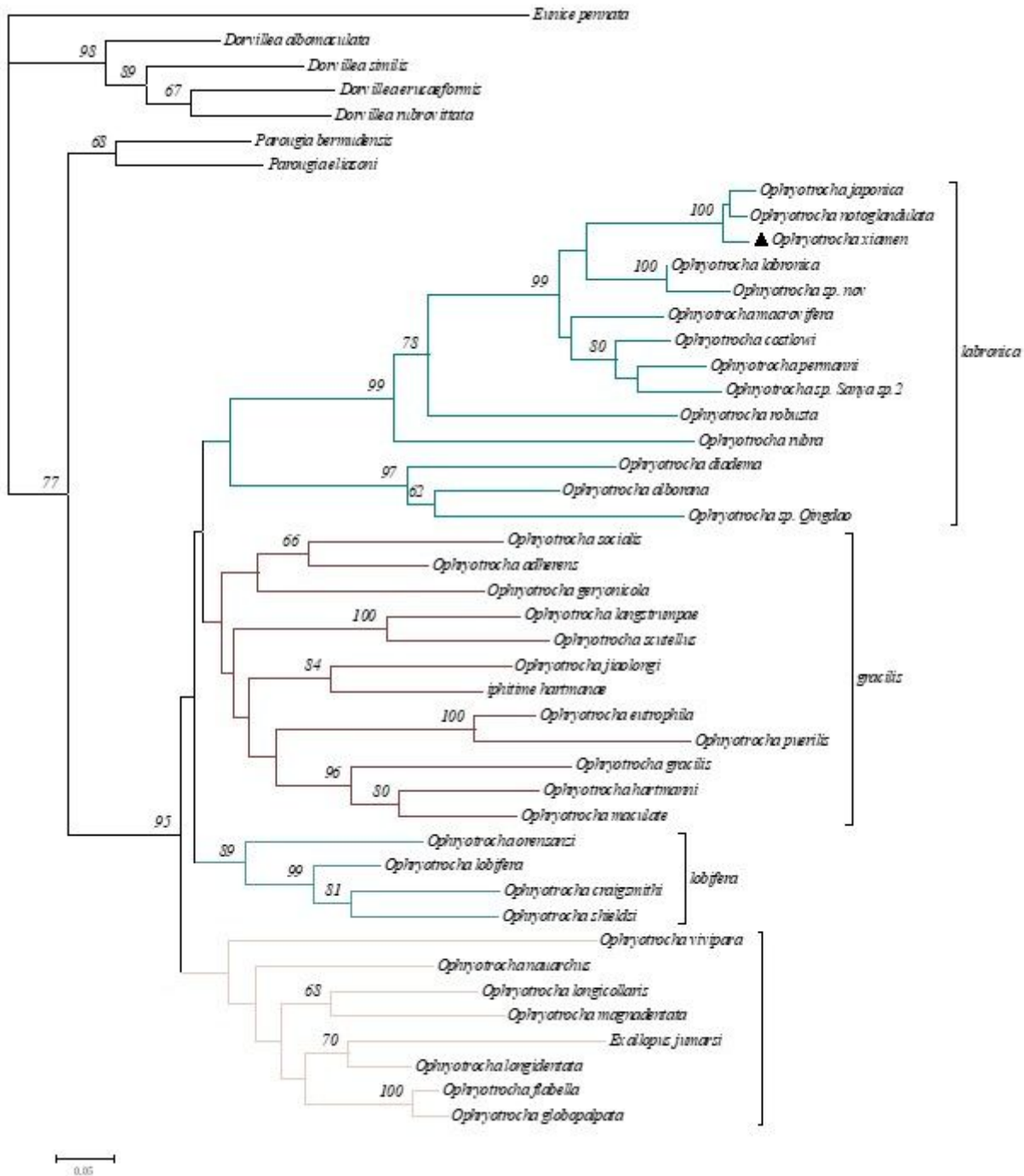


**Figure 2**

Phylogenetic analyses of a combined data set with two genes (COI and H3). The tree was calculated using maximum parsimony method (bootstrap 1000 replications). The scale bar indicates 0.05 nucleotide substitutions per site. A symbol ▲ indicate *O. xiamen* from this study.

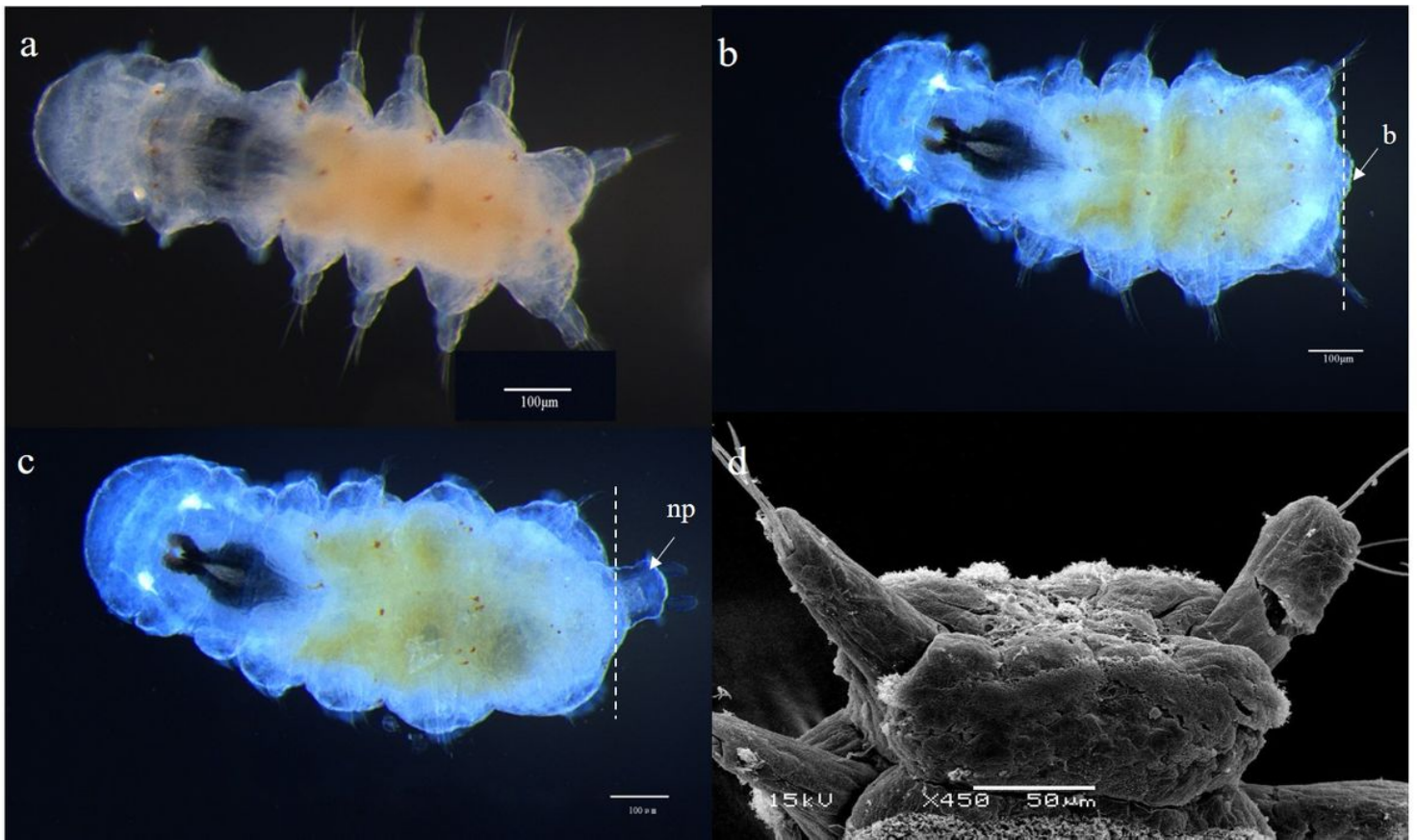


**Figure 3**

Morphological characterization of early regeneration. a, d Light microscopy and SEM images of *O. xiamen* 1-day post amputation. b 2-day post amputation. c 3-day post amputation with new pygidium. b: blastema; np: new pygidium. The dotted lines show the amputation sites. Scale bars are shown at the bottom of each images.

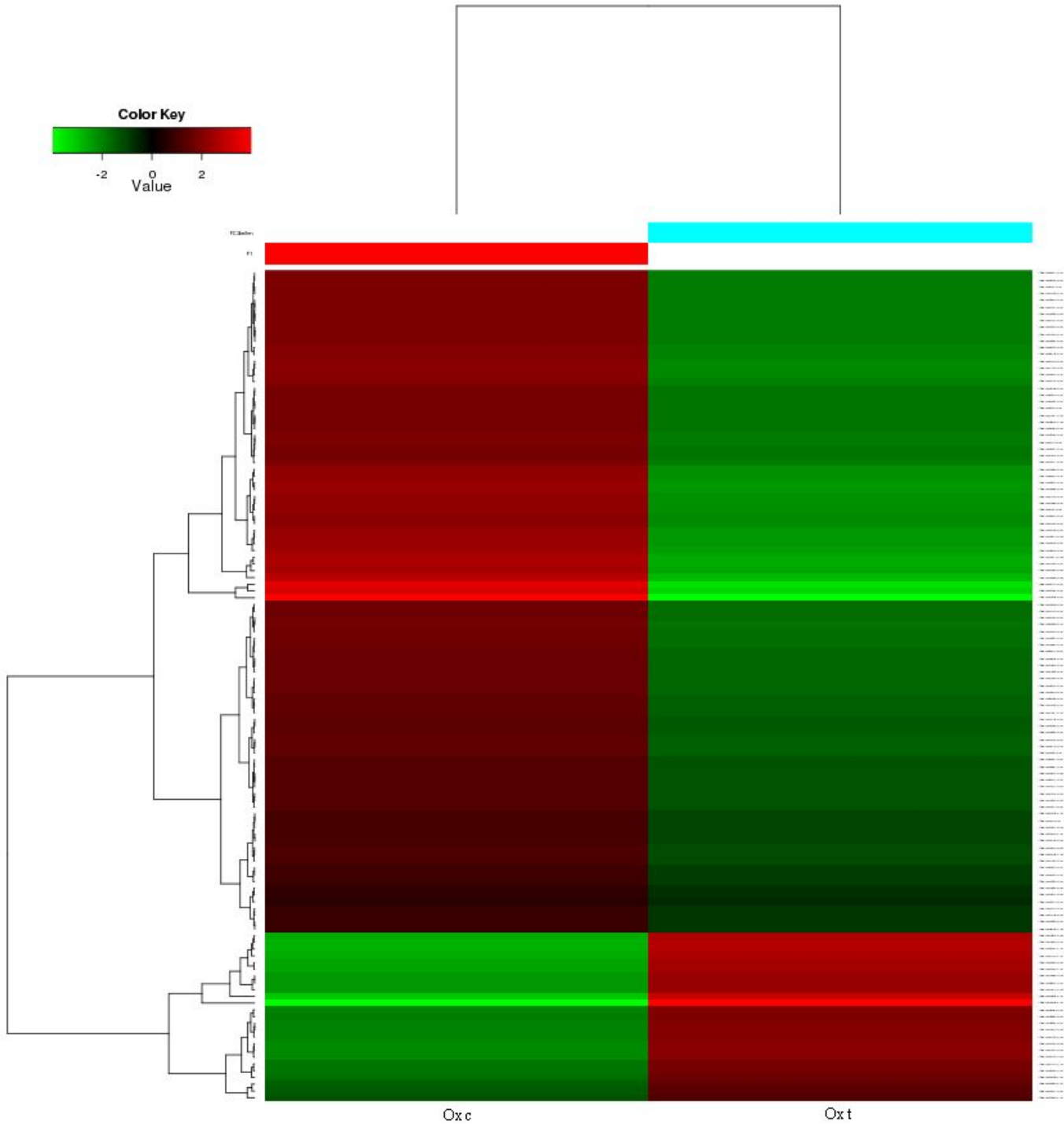


**Figure 4**

Hierarchical clustering of differentially expressed genes during early regeneration (fold change >2 and FDR < 0.05). Red color indicates up-regulated expression, whereas green color indicates down-regulated expression. Ox c: control group; Ox t: regeneration group (1 day). See Additional file 8 for detailed results.

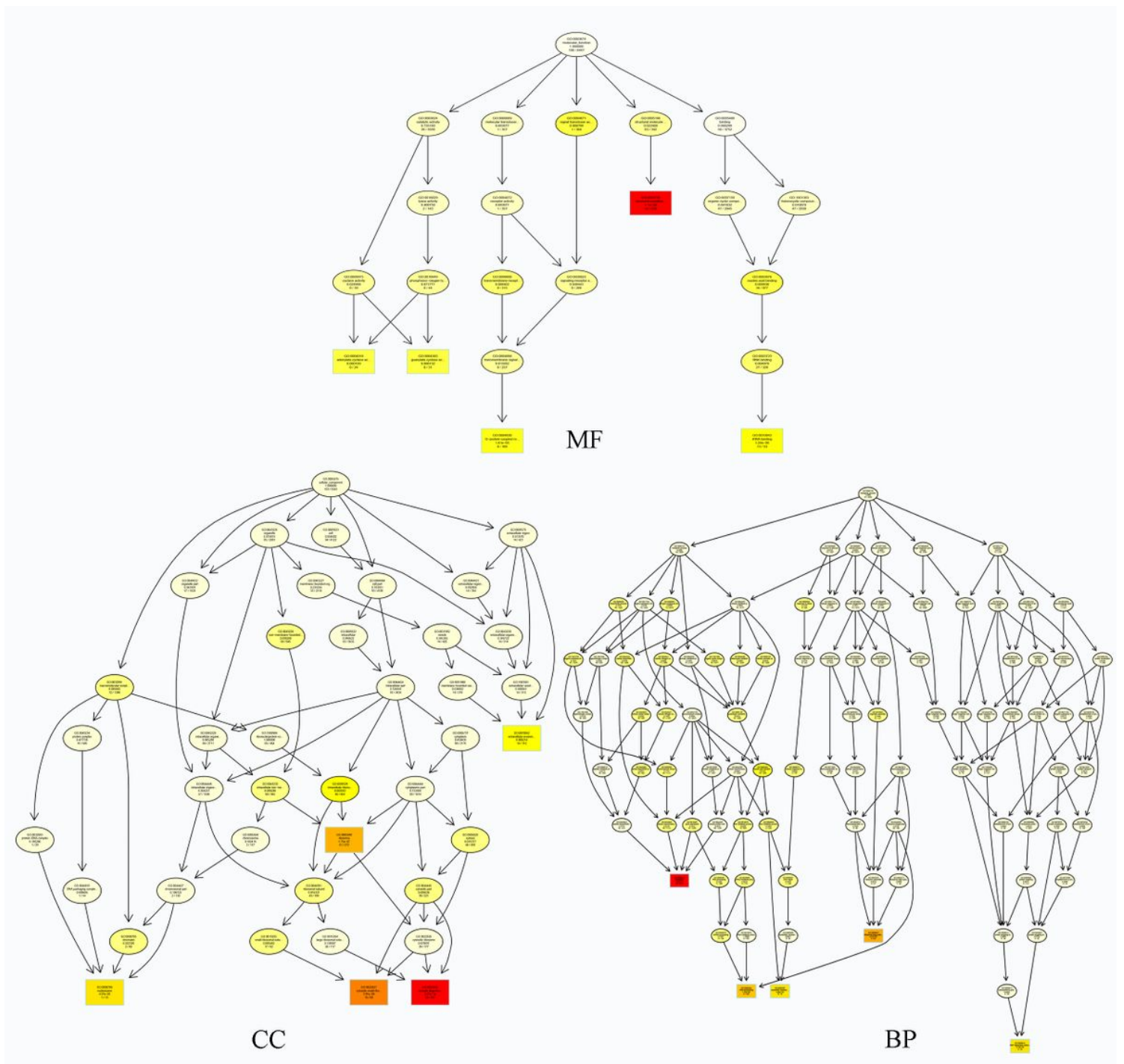


**Figure 5**

GO classification of transcripts of *O. xiamen*. The unigenes from the regeneration and control groups are classified into three main categories: Molecular Function (MF), Cellular Components (CC), and Biological Process (BP).

## Supplementary Files

This is a list of supplementary files associated with this preprint. [Click to download.](#)

- additionalfile1.jpg
- Additionalfile2.docx
- Additionalfiles3.docx
- additionalfile4.jpg
- Additionalfile5.docx
- additionalfile6.jpg
- Additionalfile7.jpg
- Additionalfile8.xlsx
- Additionalfile9.jpg
- Additionalfile10.docx